

*Phosphorescence quantum yield
enhanced by intermolecular hydrogen
bonds in Cu₄I₄ clusters in the solid state*

Article

Accepted Version

Mazzeo, P. P., Maini, L., Petrolati, A., Fattori, V., Shankland, K.
ORCID: <https://orcid.org/0000-0001-6566-0155> and Braga, D.
(2014) Phosphorescence quantum yield enhanced by
intermolecular hydrogen bonds in Cu₄I₄ clusters in the solid
state. Dalton Transactions, 43 (25). pp. 9448-9455. ISSN
1364-5447 doi: 10.1039/c4dt00218k Available at
<https://centaur.reading.ac.uk/39207/>

It is advisable to refer to the publisher's version if you intend to cite from the
work. See [Guidance on citing](#).

To link to this article DOI: <http://dx.doi.org/10.1039/c4dt00218k>

Publisher: Royal Society of Chemistry

All outputs in CentAUR are protected by Intellectual Property Rights law,
including copyright law. Copyright and IPR is retained by the creators or other
copyright holders. Terms and conditions for use of this material are defined in
the [End User Agreement](#).

www.reading.ac.uk/centaur

CentAUR

Central Archive at the University of Reading

Reading's research outputs online

Phosphorescence quantum yield enhanced by intermolecular hydrogen bonds in Cu₄I₄ clusters in the solid state†

Paolo P. Mazzeo,^a Lucia Maini,^{*a} Alex Petrolati,^a Valeria Fattori,^{*b} Kenneth Shankland^c and Dario Braga^a

Organo-copper(I) halide complexes with a Cu₄I₄ cubane core and cyclic amines as ligands have been synthesized and their crystal structures have been defined. Their solid state photophysical properties have been measured and correlated with the crystal structure and packing. A unique and remarkably high luminescence quantum yield (76%) has been measured for one of the complexes having the cubane clusters arranged in a columnar structure and held together by N–H⋯I hydrogen bonds. This high luminescence quantum yield is correlated with a slow radiationless deactivation rate of the excited state and suggests a rather strong enhancement of the cubane core rigidity bestowed by the hydrogen bond pattern. Some preliminary thin film deposition experiments show that these compounds could be considered to be good candidates for applications in electroluminescent devices because of their bright luminescence, low cost and relatively easy synthesis processes.

Introduction

Copper(I) halide complexes constitute a large family of compounds based on a relatively abundant metal element and are of photochemical and photophysical interest.^{1,11} Depending on their versatile coordination environment these compounds play a unique role in both physical and biological research and application.³ Recently there has been a surge of interest in studying these complexes, which are currently at the forefront of coordination chemistry and crystal engineering research^{12,15} as active materials for optoelectronic devices.^{16,19}

In the past few decades, new concepts for lighting and display applications have been the focus of extensive research.^{20,22} Organic Light-Emitting Diodes (OLEDs) are the most promising devices for these tasks, as they can be manufactured with low cost processes and can be purpose-built in thin, flexible and lightweight substrates.²³ Organometallic complexes based on iridium,²⁴ platinum²⁵ and osmium²⁶ are commonly used as materials in OLEDs due to their high emission quantum yield and wavelength tunability, while very

recently, copper(I) has appeared in the literature as a good candidate to replace such expensive metals for OLEDs.^{16,19,27}

Whilst the luminescence in solution in halogen-organo-copper(I) complexes has been studied for decades,^{6,8} very little work has been done on these complexes in the solid state.^{19,27,29} However, the photophysical properties of the solids could be very different from those in solution due to the molecular organization through the crystals, which can be expected to affect the energies and/or the kinetics of the excited states.^{30,32} In this respect, polymorphism (i.e. the existence of different crystal forms for the same molecular or supramolecular entity) could play a key role in determining the final photophysical properties.³²

Ford et al. extensively studied the luminescence properties of copper(I) halogen complexes having a Cu₄X₄ core with a cubane-like geometry^{6,33,36} and showed that the luminescence behaviour and the environment (solvent or rigid matrix) of the complexes are strictly related.³³

In the case of the cluster Cu₄I₄(pyridine)₄,⁴ for example (hereafter **1**), two distinct emission bands were observed in solution, whose high-energy band was attributed to a triplet halide-to-ligand charge transfer (³XLCT), while the low-energy emission band was attributed to a triplet Cu–I cluster-centred (³CC) excited state with the excitation localized to the Cu₄I₄ core, only possible in the presence of an interaction between the metal centres.³⁷

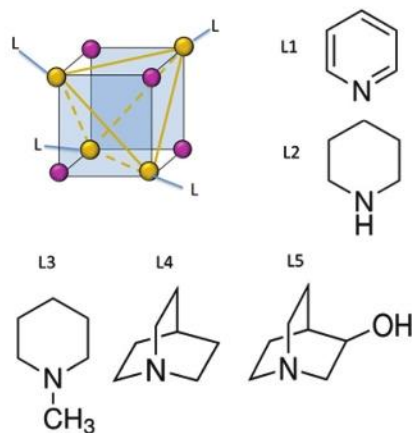
The ³CC emission band was shown to display a peculiar sensitivity to the temperature and rigidity of the medium.³⁸

^aDipartimento di Chimica "G. Ciamician", Università di Bologna, Via Selmi 2, 40126 Bologna, Italy. E-mail: l.maini@unibo.it

^bIstituto per la Sintesi Organica e la Fotoreattività (ISOF) - CNR, Via Gobetti 101 40129 Bologna, Italy. E-mail: valeria.fattori@isof.cnr.it

^cSchool of Pharmacy, University of Reading, Whiteknights, Reading RG6 6AD, UK

† Electronic supplementary information (ESI) available. CCDC 975300, 989490–989492. For ESI and crystallographic data in CIF or other electronic format see DOI: 10.1039/c4dt00218k



Scheme 1 General representation of a $\text{Cu}_4\text{I}_4\text{L}_4$ cubane cluster (yellow = copper; purple = iodine); L1 = pyridine, L2 = piperidine, L3 = N-methylpiperidine, L4 = quinuclidine, L5 = 3-quinuclidinol.

In this paper we aim to gain insight into the correlation between the photophysics and structure of $\text{Cu}_4\text{I}_4\text{L}_4$ cubane complexes in which every copper ion binds to three iodide atoms and then completes its first coordination sphere with a N-based ligand such as pyridine (L1), piperidine (L2), N-methylpiperidine (L3), quinuclidine (L4), or 3-quinuclidinol (L5) (see Scheme 1).

Apart from pyridine, we considered only saturated ligands with the aim of excluding the photophysical process involving the ligand's π system and determining which parameters affect the cluster-centred characteristics such as basicity, ability to form hydrogen bonds, and different groups bonded to the coordinating nitrogen. The different pK_b values allow to determine whether the emission quantum yield in the solid state is related to the bond strength between ligands and copper atoms.

The substitution of hydrogen with a methyl group on the coordinating nitrogen atom will allow us to determine whether the CC excited state radiationless deactivation due to the N-H bending modes coupling, as hypothesized in solution,³³ can be removed.

Moreover, the ligands show a progressive rigidity and a different ability to form H-bonds and consequently allow to investigate how the vibrations involving the ligand σ backbone can influence the photophysical properties of the complexes. Some preliminary thin film deposition experiments have been carried out in order to predict the applications of these complexes in solid-state optoelectronic devices.

Results and discussion

Six tetrakis($(\mu_3\text{-Iodo})\text{-ligand-copper(II)}$) cubane complexes have been synthesized: $\text{Cu}_4\text{I}_4\text{pyridine}_4$ (1), $\text{Cu}_4\text{I}_4\text{piperidine}_4$ (2), $\text{Cu}_4\text{I}_4\text{N-methylpiperidine}_4$ (3), $\text{Cu}_4\text{I}_4\text{quinuclidine}_4$ (4) and two crystal forms of $\text{Cu}_4\text{I}_4(3\text{-quinuclidinol})_4$ (5a and 5b).

For all complexes, the crystal structure and photophysical properties in the solid state have been measured. Complexes 1 and 2 have already been studied and their crystal structure and photophysical data (apart from solid state emission quantum yields) have been reported,^{4,33,38,39} while 3, 4, 5a and 5b are accounted here for the first time.

Synthesis and crystal structures

Compounds 1 and 2 were obtained as crystalline powders by following the previously reported synthesis, while 3, 4, 5a and 5b were obtained by modification of the previously reported synthesis. Single crystals of 3, 4, and 5b were obtained by triple layer crystallization (see the Experimental part). While no single crystal suitable for SCXR analysis of 5a could be obtained, its structure has been determined from X-ray powder diffraction data via Rietveld refinement of a starting model derived from the single-crystal coordinates of 4 as we found that the two structures are isomorphous (see below).

The crystal structures of 1–5 are characterized by the presence of distorted cubane clusters (see Fig. 1) and in all compounds the Cu-Cu distances are compatible with metallophilic interactions as, inside the Cu_4I_4 clusters, they are shorter than two times the van der Waals radius of Cu which has been recently evaluated as 1.92 \AA ^{40,41} (see Table 1). The ligand molecules are located on the vertex of the tetrahedral coordinating copper atoms as a sort of blades.

In compounds 1, 2 and 3 the complexes are piled up to form columns which run parallel to one another (see Fig. 2). In compound 1 only weak C-H $\cdots\pi$ interactions are present among the discrete entities, while compound 2 is characterized by the presence of intermolecular hydrogen bonds. The hydrogen atoms belonging to the nitrogen point to the iodine atoms of an adjacent cluster and form N-H \cdots I interactions. Evidence of the hydrogen bond comes from the alignment of the N-H-I atoms ($159^\circ(1)$) and the H-I distance ($2.935(3) \text{ \AA}$) which is shorter than the sum of the atomic radii (3.16 \AA).⁴² Since the clusters are piled up, each cubane cluster is pinched by eight hydrogen bonds, four on one side and four on the opposite side (see Fig. 2b).

In compound 3 the Cu-Cu distances are about $2.868(3) \text{ \AA}$ and $2.946(2) \text{ \AA}$, slightly longer than the other compounds, but

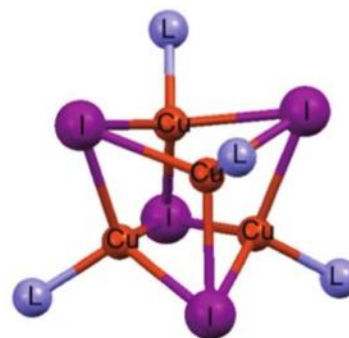


Fig. 1 Distorted cubane cluster with nitrogen atoms belonging to the ligand coordinating the copper atoms.

Table 1 Interatomic distances in Cu₄I₄ clusters

	Cu-Cu (Å)	Cu-I (Å)	I-I (Å)
1	2.619(2)	2.630(4)	2.697(4)
	2.684(6)	2.665(3)	2.701(4)
	2.689(3)	2.669(6)	2.720(7)
	2.707(8)	2.670(3)	2.733(2)
	2.719(4)	2.677(5)	2.790(2)
	2.721(1)	2.692(3)	2.794(4)
2	2.595(5)	2.682(3)	4.443(7)
	2.640(1)	2.687(3)	4.478(8)
		2.711(4)	4.488(2)
3	2.868(3)	2.690(1)	4.513(2)
	2.946(2)	2.696(4)	4.529(4)
		2.683(2)	4.594(2)
4	2.671(2) ^a	2.669(2) ^a	4.473(3)
	2.696(3) ^a	2.685(8) ^a	4.584(1)
	2.725(3) ^b	2.695(1) ^a	4.459(2) ^a
		2.682(2) ^b	4.493(1) ^a
5a	2.695(2) ^a	2.692(2) ^a	4.456(1) ^b
	2.720(2) ^a	2.709(3) ^a	4.498(1) ^a
	2.749(3) ^b	2.719(5) ^a	4.533(2) ^a
		2.706(7) ^b	4.496(3) ^b
5b	2.648(3)	2.661(3)	2.696(4)
	2.660(2)	2.679(6)	2.699(6)
	2.662(4)	2.683(3)	2.704(3)
	2.705(4)	2.688(8)	2.715(2)
	2.706(2)	2.689(7)	2.717(4)
	2.745(1)	2.692(2)	2.721(1)

^{a, b} Referred to crystallographic independent cubane clusters in the structure.

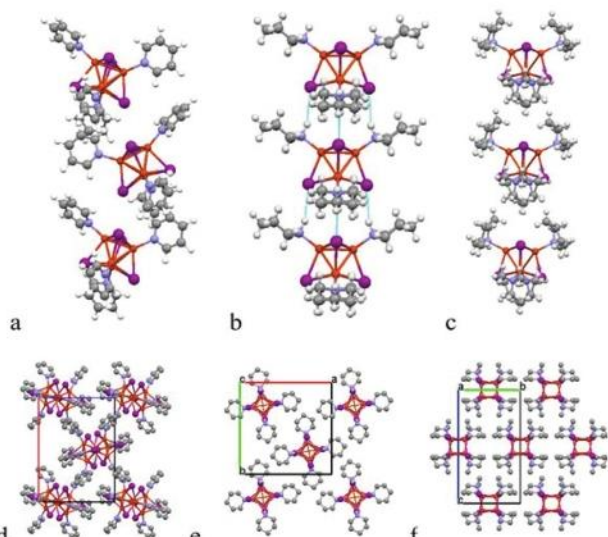


Fig. 2 The columns of cubane moieties in compounds 1 (a), 2 (b) and 3 (c) and how they pack in the crystal structures 1 (d), 2 (e) and 3 (f). In 2 (b) the N-H...I hydrogen bonds are highlighted in blue. In d, e, f, hydrogen atoms are omitted for the sake of clarity.

it seems not to affect the photophysical properties. As for 2, in compound 3 the cubane clusters are piled up in columns, but the tertiary nitrogen atom of the N-methylpiperidine rules out the formation of hydrogen bond interactions among the cubane complexes.

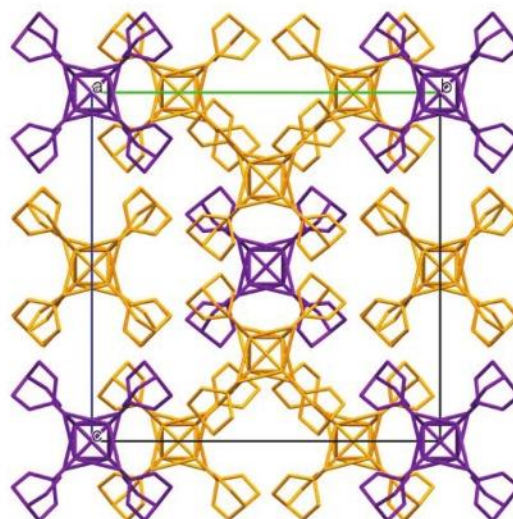


Fig. 3 Crystal structure of 4. The two independent cubane moieties are coloured in purple and orange. Hydrogen atoms are omitted.

Compound 4 crystallizes with a cubic lattice and is characterized by two different cubane moieties that are not symmetry related. In the structure, one asymmetric cluster occupies the node and the centre of the cell while the second asymmetric cluster is located on the face. This particular arrangement prevents the formation of columns observed in the previous structures (Fig. 3).

Two crystal forms 5a and 5b have been obtained by reacting CuI with quinuclidinol. Single crystals of 5a could not be obtained, but its powder X-ray diffraction pattern shows it to be isomorphous with structure 4 (Fig. 4). The unit cell parameter of 5a was easily refined using the cell parameter of 4 as the starting point.

The structure of 5a was then solved from the powder data using, as the initial coordinates for rigid-body Rietveld refinement, the structure of the compound 4 conveniently modified

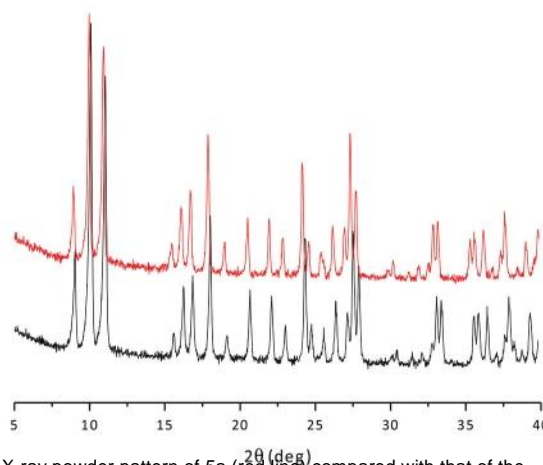


Fig. 4 X-ray powder pattern of 5a (red line) compared with that of the isomorphous compound 4 (black line).

by changing the H atoms into O-H groups in positions 3, 5 and 8 with respect to N in the quinuclidinol ligand with 1/6 occupancy (because of the rotation along C_3 and of the chirality of the ligand in those positions).

The position of the hydroxyl groups is disordered and although the hydroxyl groups belonging to different clusters could form hydrogen bonds, a hydrogen bond pattern cannot be identified.

Compound **5b** presents the same complex units as **5a** and, in this case, the hydroxyl groups are disordered mainly over two positions. The $Cu_4I_4L_4$ can be described as triangular based pyramids, which are arranged in layers with the parallel bases to form a flat side while the opposite side is characterized by the presence of the vertex of the pyramids. The layers face one another in a complementary way and form curvy monodimensional channels in which disordered solvent molecules are trapped (see Fig. 5). The presence of solvent molecules in the crystal structure has been confirmed by TGA analysis (see ESI†).

Conversions

A variable temperature XRPD analysis has been performed on **5b** with in situ characterization of the powder. As shown in Fig. 6, on heating up the powder to 100 °C, loss of crystallinity

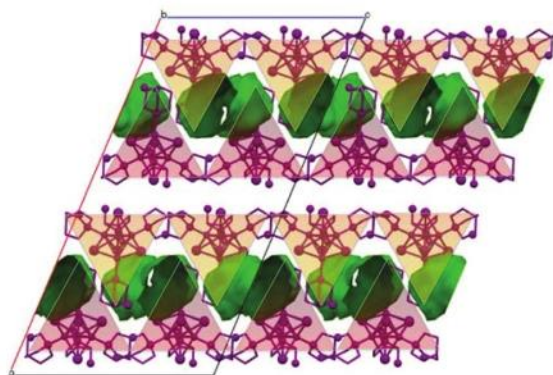


Fig. 5 Voids analysis in compound **5b**. Hydrogen atoms are removed for clarity. Curvy monodimensional channels (\varnothing 8.57 Å) are present in the structure along the b-axis. The cubane moieties are packed along the bc plane like pyramidal blocks in complementary sound absorbing panels.

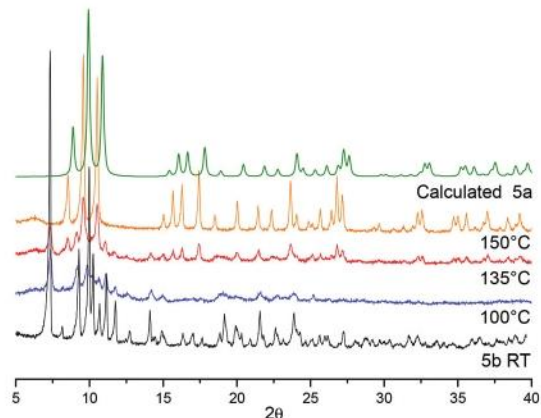


Fig. 6 Variable temperature XRPD analysis performed on **5b**, 100 °C: loss of crystallinity due to the solvent release; 135 °C (blue line): appearance of the **5a** phase at 135 °C (red line) and complete conversion to form **5a** at 150 °C (orange line). The green line is the calculated pattern of **5a** based on the structure solved at RT. The peak's shift of the orange pattern is ascribable to the cell expansion for the high temperature.

is observed due to the release of the disordered solvent molecules trapped into the channels (see ESI†). At 135 °C, peaks of the **5a** phase appear in the diffractogram while the peak intensities of the **5b** phase decrease. A **5b** to **5a** polymorphic conversion is complete at 150 °C. After cooling down to ambient temperature no recovery of the **5b** phase occurs and the phase **5a** remains stable.

Photophysical properties

All complexes have been characterized by recording excitation and emission spectra and measuring luminescence quantum yields and lifetimes in the solid state. The photophysical data are reported in Table 2. Luminescence behaviour in solution was not investigated since our aim was to evaluate the effect of the crystal structure on the photophysical properties. Moreover, all complexes are poorly soluble and their emission properties are expected to be largely depressed in solution as proved by the big drop in the luminescence quantum yield for **1** and **2** in solution (Table 2, in parentheses, taken from the literature⁴) as a consequence of a big distortion of the excited state with respect to the ground state, which is also the reason

Table 2 Photophysical parameters for compounds **1–5b** as powders at room temperature. In brackets toluene solution data from the literature⁴

	λ_{exc}^b (nm) _{max}	λ_{em}^c (nm) _{max}	Stokes shift (cm ⁻¹)	Φ	τ^d (μs)	k_f (10 ⁴ s ⁻¹)	k_{nr} (10 ⁴ s ⁻¹)
1	360	570 (690)	10 200	0.51 (0.09)	10.5 (10.6)	4.9 (0.8)	4.7 (8.6)
2	370	570 (680)	9500	0.76 (0.0002)	12.3 (0.11)	6.2 (0.2)	2.0 (910)
3	330	560	12 400	0.44	10.6	4.2	5.3
4	330	540	11 800	0.50	14.2	3.5	3.5
5a	350	550	10 400	0.48	14.5	3.3	3.6
5b^a	350	565	10 900	0.30	10.3	2.9	6.8
5b	340	565	11 700	0.15	9.8	1.5	8.7

^a Data related to compound **5b** once heated at 80 °C and then cooled down to ambient temperature. ^b Excitation maxima, data recorded at maximum emission wavelength. ^c Emission maxima, excitation at 350 nm. ^d Lifetimes, excitation at 331 nm. The kinetic constants k_f and k_{nr} were calculated using the equations $k_f = \Phi/\tau$ and $k_{nr} = (1 - \Phi)/\tau$.

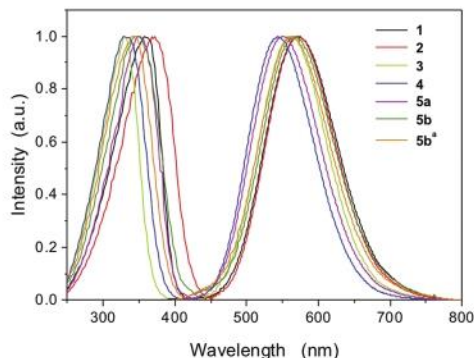


Fig. 7 Normalized excitation spectra (250-450 nm, excitation at the emission maximum) and emission spectra (400-800 nm, λ_{exc} = 350 nm). All measurements were done on powders at room temperature.

for the large red shift of the emission band. The fast radiation-less deactivation of the excited state in solution, represented by the high value of the decay constant k_{nr} (Table 2), remarkably high for 2, is associated with an efficient coupling of the ligand vibrations with the electronic transition.³³

Apart from 1, having an unsaturated ligand whose π^* orbitals are involved in the excitation conferring an ¹XLCT character on the transition, the excitation spectra of all the other complexes are characterized by an envelope of bands extending below 400 nm which are associated with so-called "cluster centred" (¹CC) electronic transitions which go from HOMOs, localized mainly on the iodide lone pairs, to LUMOs having Cu-Cu bonding and Cu-I antibonding character^{37,43} (Fig. 7). The emission bands have their maxima between 540 nm and 570 nm associated with radiative decay from cluster-centred triplet states (³CC) characterized by lifetimes in the 10-15 μ s range and highly distorted with respect to the ground state geometry as shown by lack of vibrational structure and large Stokes shifts.³⁷ This picture is consistent with cuprophilic interactions, which are compatible with Cu-Cu distances inside the Cu_4I_4 clusters shorter than two times the van der Waals radius of Cu which has been recently evaluated as 1.92 Å.^{40,41} Even the rather long Cu-Cu distances in 3 (2.868 Å; 2.946 Å) do not prevent metal-metal interactions and ³CC emission.

However, despite having similar origins, the luminescence transitions occur with different quantum yields for the different compounds.

Their values are in the 40-50% range for most complexes, but a rather higher value for 2 (76%) and a somewhat lower value for 5b (30%) have been measured. The quantum yield is dramatically increased compared to the data reported for 1 and 2 in solution; this behaviour agrees with an increase of the luminescence intensity upon stiffening of the local environment. The quantum yield trend seems to correlate fairly well to the radiationless decay rate constant (k_{nr}) which has the lowest value for 2. Only for this complex the crystalline structure highlights the presence of N-H...I hydrogen bonds between adjacent clusters that assures rigidity to the Cu_4I_4 cubane core,

preventing vibrations that promote non-radiative decay of the excited state. Thus, while 2 in solution has an extremely low quantum yield, it jumps to the highest values as a solid.

The cubane rigidity of this complex has some effect also on the radiative decay constant (k_r), which is the highest one, and on the Stokes shift (9500 cm^{-1}) which is lower than the other cluster values ranging from 10 200 to 12 400 cm^{-1} . Both the effects can be correlated to a lower distortion of the excited state with respect to the ground state as a direct consequence of the N-H...I hydrogen bond which enhances the cubane core stiffness.

Accordingly, the more flexible crystal structure of 5b affects both k_r and k_{nr} , resulting in a lower luminescence quantum yield. An even lower value has been measured after heating at 80 °C and cooling down to room temperature the powder (5b^a in Table 2), as the desolvation process leads to loss of crystallinity.

The two isomorphous complexes 5a and 4 show similar quantum yields and kinetic constants.

Thin films

Direct deposition of the complex onto film was unsuccessful due to the degradation of the complex at high temperature and low pressure. Having stated that a solid-vapour reaction occurred when the copper iodide crystalline powder was exposed to the ligand vapours at room temperature, the same reaction was attempted with a CuI thin film. A thin copper iodide layer was deposited onto a polished glass slide by high-vacuum sublimation obtaining a polycrystalline, uniform, and smooth layer which showed the characteristic X-ray diffraction (111) peak of the γ phase. Then, the CuI film was exposed to the vapours of the ligand into a closed chamber until complete reaction, as suggested from the absence of any CuI peak in the XRPD analysis (see ESI†). Our best results have been obtained by exposing a 35 nm thick CuI layer to the vapours of quinuclidine and of 3-quinuclidinol at room temperature. The X-ray diffraction analysis directly performed in the Bragg-Brentano geometry on these films shows that they are both amorphous. The photoluminescence spectra of both films are in agreement with the emission spectra of the 4 and 5a powders respectively. A sample obtained by reacting the CuI film with quinuclidine and showing a green luminescence when exposed to UV radiation ($\lambda = 365$ nm) is reported in Fig. 8.

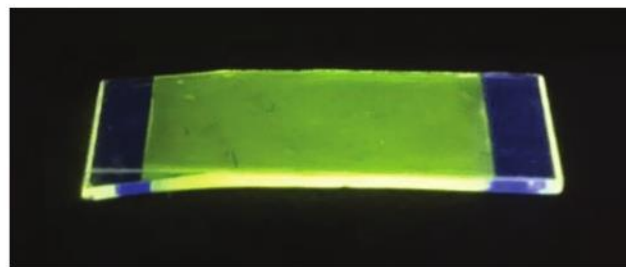


Fig. 8 Picture of CuI deposited onto a silica glass slide after exposition to vapour of quinuclidine under 365 nm UV lamp irradiation.

When the CuI films were exposed to piperidine and N-methylpiperidine vapours the reaction was too fast due to the higher vapour pressures of these ligands and the samples resulted as blotched and not uniformly emissive layers. More trials are in progress in order to improve the film uniformity by carefully controlling the solid-vapour reaction.

Experimental section

General

All glassware was dried in an oven set to a temperature of 80 °C for 24 h prior to use. All reagents were purchased from Sigma Aldrich and used without further purification.

Photophysics

All determinations made use of powder samples placed between two quartz slides and were done at room temperature. Excitation and emission spectra were obtained with a SPEX Fluorolog fluorometer; excitation spectra were monitored at the maximum emission wavelength and emission spectra were recorded exciting all samples at 350 nm. Absolute photo-luminescence quantum yields were measured according to the method of deMello,⁴⁴ by using an integrating sphere customized to fit into the SPEX fluorometer sample compartment. The estimated error on the quantum yield is 10%. Luminescence lifetimes were measured with an IBH 5000F time-correlated single-photon counting apparatus, by using a pulsed NanoLED excitation source at 331 nm. Analysis of the luminescence decay profiles was accomplished with the Decay Analysis Software DAS6 provided by the manufacturer, with an estimated error on the lifetimes of 5%. All decays were monoexponential. The kinetic constants k_r and k_{nr} were calculated using the equations $k_r = \Phi/\tau$ and $k_{nr} = (1 - \Phi)/\tau$.⁴⁵

X-Ray powder diffraction

X-Ray powder diffractograms were collected on a Panalytical X'Pert PRO automated diffractometer with CuK α radiation and an X'Celerator equipped with an Anton Paar TTK 450 low-

temperature camera. The program Mercury⁴⁶ was used for the calculation of X-ray powder patterns.

PXRD data of **5a** were collected over the range 3–70° 2 θ (2 kW; Cu-K α , 1.54056 Å step size 0.017 2 θ), using a variable count time scheme.⁴⁷ The Bruker D8 Advance diffractometer was equipped with a LynxEye detector. The data set was background subtracted and truncated to 50° 2 θ for Pawley fitting ($\chi^2 = 1.9$). A scale-only Rietveld refinement against the original data was set in the range 4°–65° 2 θ to give a good final fit, $R_{wp} = 2.89$.

Crystal structure determination

Crystal data for **3–4** and **5b** were collected on an Oxford Xcalibur S with MoK α radiation, $\lambda = 0.71073$, monochromator graphite and equipped with a liquid nitrogen Oxford-Cryo-stream device. Crystal data and details of measurements are summarized in Table 3. SHELX97⁴⁸ was used for the structure solution and refinement based on F². Non-hydrogen atoms were refined anisotropically. The asymmetric unit of compound **3** consists of 1/8 of the chemical formula [Cu₄I₄(NC₆H₁₃)₄]. The atoms Cu1, I1, N1, C3 and C4 lay on the mirror plane. The asymmetric unit of compound **4** consists of two different cubane moieties. One moiety has the formula [CuI(NC₇H₁₃)] and all atoms are in general position while the second one has the formula [CuI(NC₇H₁₃)]_{0.3} and the atoms Cu2, I4, N2 and C10 lay on the 3-fold axes. The Mercury⁴⁶ software package was used for the graphical representation of the resulting structures.

Synthesis of compound 1. CuI (1 mmol, 0.190 g) was dissolved in the minimum amount of a saturated aqueous solution of KI (≈ 2 mL). While stirring, pyridine (1.2 mmol, 0.01 mL) was added. The product precipitated instantly as a whitish powder that gave yellow emission under UV/Vis radiation. The solid material was recovered by filtration on a Buchner funnel and washed with saturated KI aqueous solution and bi-distilled water. Once recovered, the powder has been dried in a desiccator with silica gel.

Synthesis of compound 2. CuI (1 mmol, 0.190 g) was dissolved in a minimum amount of a saturated aqueous solution

Table 3 Crystallographic data of compounds 1–5

	1 ⁴⁹	2 ⁵⁰	3	4	5a ^a	5b
Empirical formula	C ₂₀ H ₂₀ Cu ₄ I ₄ N ₄	C ₂₀ H ₄₄ Cu ₄ I ₄ N ₄	C ₂₄ H ₅₂ Cu ₄ I ₄ N ₄	C ₂₈ H ₅₂ Cu ₄ I ₄ N ₄	C ₂₈ H ₅₂ Cu ₄ I ₄ N ₄ O ₄	C ₂₈ H ₅₂ Cu ₄ I ₄ N ₄ O ₄
Formula weight	1098.4	1102.39	1158.46	1206.50	1270.50	1270.50
Temperature	293(2) K	293(2) K	293(2) K	293(2) K	293(2) K	293(2) K
Wavelength	0.71073	0.71073	0.71073	0.71073	1.54056	0.71073
Crystal system	Orthorhombic	Tetragonal	Tetragonal	Cubic	Cubic	Monoclinic
Space group	P2 ₁ 2 ₁ 2 ₁	P4 ₂ /n	I42m [–]	P43n [–]	P43n [–]	C2/c
Unit cell dimensions	a = 16.032(6) b = 15.510(2) c = 11.756(3) $\beta = 90$	a = 14.589(1) b = 14.589(1) c = 7.538(1)	a = 9.9963(7) b = 9.9963(7) c = 18.114(2) $\beta = 90$	a = 19.7281(6) b = 19.7281(6) c = 19.7281(6) $\beta = 90$	a = 19.9029(2) a = 19.9029(2) a = 19.9029(2) $\beta = 90$	a = 37.444(4) b = 12.2662(8) c = 20.000(2) $\beta = 113.38(1)$
Volume	2923.2	1604.7	1810.1(3)	7678.1(4)	7884.0(3)	8431(1)
Z	2	2	2	8	8	8
CCDC number/ref. code	CUIPYR	CUIPIP	975399	975300	975301	975302

^a Data obtained from Rietveld refinement on powder diffraction pattern.

of KI (≈ 2 mL). While stirring, piperidine (1.2 mmol, 0.008 mL) was added. The product precipitated instantly as a whitish powder that gave yellow emission under UV/Vis radiation. The solid material was recovered by filtration on a Buchner funnel and washed with saturated KI aqueous solution and bi-distilled water. Once recovered, the powder has been dried in a desiccator with silica gel.

Synthesis of compound 3. CuI (5 mmol, 0.950 g) were added as solid to 2 mL of methyl-piperidine. After 3 days, during which time the suspension had been taken under stirring at room temperature in a closed flask, the product was filtered on a Buchner funnel and washed with an aqueous saturated solution of KI and bi-distilled cold water. Once recovered, the powder, which gave green emission under UV/Vis radiation, was dried in a desiccator with silica gel. The title compound was also obtained after 10 minutes of grinding, in an agate mortar, 0.190 g of CuI (1 mmol) with a few drops of methyl-piperidine. As the ligand is liquid and volatile at rt, the title compound was obtained also via exposure of CuI to vapour of methyl-piperidine after 2 days. Single crystals were obtained by a three-layer crystallization: the lower layer was CuI dissolved in saturated aqueous solution of KI; the middle layer was pure ethanol and the top layer was a solution of methyl-piperidine in acetone. Crystals appeared after 5-7 days and were chosen with the help of a UV lamp.

Synthesis of compound 4. CuI (0.095 g, 0.5 mmol) was dissolved in a minimum amount of a saturated aqueous solution of KI (≈ 2 mL). While stirring, a solution of quinuclidine (0.068 g, 0.6 mmol) in ethanol (1 mL) was added. The product precipitated instantly as a whitish powder with green emission under UV/Vis radiation. The solid material was recovered by filtration on a Buchner funnel and washed with saturated KI aqueous solution and bi-distilled water. Once recovered, the powder was dried in a desiccator with silica gel.

Single crystals were obtained by three-layer crystallization: the lower layer was CuI dissolved in saturated aqueous solution of KI; the middle layer was pure ethanol and the top layer was a solution of quinuclidine in n-hexane.

Synthesis of compound 5a. Racemic 3-quinuclidinol (0.127 g, 1.2 mmol) was dissolved in methanol (1 mL) at 80 °C and was added, under stirring, to a saturated KI aqueous solution of CuI (0.190 g, 1 mmol) at 80 °C. The product was precipitated as a fine white powder, with green emission under UV/Vis radiation; the solid material was recovered by filtration with a Buchner funnel and washed with saturated KI aqueous solution and bi-distilled water. Once recovered, the powder was dried in a desiccator with silica gel.

Synthesis of compound 5b. CuI (1 mmol, 0.190 g) were added as solid into a flask filled with a solution of racemic 3-quinuclidinol (1 mmol, 0.127 g) in methanol (4 mL). 24 hours later the product was filtered on a Buchner funnel and washed with an aqueous saturated solution of KI and bi-distilled cold water. Once recovered, the powder was dried in a desiccator with silica gel. The title compound was also obtained after several hours of grinding in a ball milling a 1 : 1 physical mixture of the reagents with a catalytic amount of

ethanol. Single crystals were obtained by three-layer crystallization: the lower layer was CuI dissolved in saturated aqueous solution of KI; the middle layer was pure ethanol and the top layer was a solution of 3-quinuclidinol in water. Crystals appeared after 5-7 days and were chosen with the help of a UV lamp.

Conclusions

Two known (1 and 2) and four new (3, 4, 5a and 5b) tetrakis-((μ_3 -iodo)-ligand-copper(I)) cubane complexes have been synthesized as crystalline powders and their photophysical properties have been measured. The crystal structures of 3, 4, 5b have been determined by single crystal X-ray diffraction while 5a was solved from the powder data.

All complexes show a cubane Cu_4I_4 core and are luminescent due to radiative decay of a cluster centred ^3CC emitting state. Quantum yields are in the range of 40-50% for all complexes apart from a slightly lower 30% for 5b and a significantly higher value of 76% for 2 which, to the best of the authors' knowledge, has never been demonstrated previously for cubane complexes. No significant interactions between the constituting moieties are observed in the crystal structures of the complexes except for compound 2 where the clusters are held together by hydrogen bonds in pillars. It results that each cluster is involved in eight hydrogen bonds, and clusters are aligned along the c-axis to build a stiff columnar structure. We think that these interactions make the cluster extremely rigid and allow to get a very high luminescence quantum yield. On the other hand, the less rigid structure of 5b results in the lowest quantum yield (30%). Desolvation of 5b leads to loss of crystallinity which results in an even more reduced quantum yield (15%).

Some preliminary attempts to obtain thin films of the pure complexes have been made by using solid-vapour reactions and some uniformly luminescent samples have been obtained. These results may be a first indication of the possibility of application of these complexes as emissive layers in electroluminescent devices, as they do not suffer from concentration quenching and have emissive triplet excited states which are compliant with the "triplet harvesting" frame for high efficiency OLEDs.

Acknowledgements

We thank MIUR, University of Bologna and CNR for financial support of this research. PPM thanks the University of Bologna for a PhD grant and the Marco Polo fellowship for supporting his visiting period at Reading University.

Notes and references

- 1 F. G. Mann, D. Purdie and A. F. Wells, *J. Chem. Soc.*, 1936, 447-460.
- 2 G. Tartarini, *Gazz. Chim. Ital.*, 1933, 63, 597-600.

- 3 N. Armaroli, G. Accorsi, F. Cardinali and A. Listorti, in *Photochemistry and Photophysics of Coordination Compounds I*, ed. V. Balzani and S. Campagna, Springer-Verlag, Berlin, 2007, vol. 280, pp. 69-115.
- 4 K. R. Kyle, C. K. Ryu, P. C. Ford and J. A. DiBenedetto, *J. Am. Chem. Soc.*, 1991, **113**, 2954-2965.
- 5 P. C. Ford and A. Vogler, *Acc. Chem. Res.*, 1993, **26**, 220-226.
- 6 P. C. Ford, *Coord. Chem. Rev.*, 1994, **132**, 129-140.
- 7 H. D. Hardt and A. Pierre, *Inorg. Chim. Acta*, 1977, **25**, L59-L60.
- 8 H. D. Hardt, H. Gechnizdjani and A. Pierre, *Naturwissenschaften*, 1972, **59**, 363.
- 9 H. D. De Ahna and H. D. Hardt, *Z. Anorg. Allg. Chem.*, 1972, **387**, 61-71.
- 10 P. C. Ford, E. Cariati and J. Bourassa, *Chem. Rev.*, 1999, **99**, 3625-3648.
- 11 H. D. Hardt and A. Pierre, *Naturwissenschaften*, 1975, **62**, 298.
- 12 P. P. Mazzeo, L. Maini, D. Braga, G. Valenti, F. Paolucci, M. Marcaccio, A. Barbieri and B. Ventura, *Eur. J. Inorg. Chem.*, 2013, **2013**, 4459-4465.
- 13 C. H. Arnby, S. Jagner and I. Dance, *CrystEngComm*, 2004, **6**, 257-275.
- 14 R. Peng, S. R. Deng, M. Li, D. Li and Z. Y. Li, *CrystEngComm*, 2008, **10**, 590-597.
- 15 S. Q. Bai, J. Y. Kwang, L. L. Koh, D. J. Young and T. S. A. Hor, *Dalton Trans.*, 2010, **39**, 2631-2636.
- 16 Z. Liu, M. F. Qayyum, C. Wu, M. T. Whited, P. I. Djurovich, K. O. Hodgson, B. Hedman, E. I. Solomon and M. E. Thompson, *J. Am. Chem. Soc.*, 2011, **133**, 3700-3703.
- 17 Z. Liu, P. I. Djurovich, M. T. Whited and M. E. Thompson, *Inorg. Chem.*, 2011, **51**, 230-236.
- 18 S. Perruchas, X. F. L. Gof, S. Maron, I. Maurin, F. o. Guillen, A. Garcia, T. Gacoin and J.-P. Boilot, *J. Am. Chem. Soc.*, 2010, **132**, 10967-10969.
- 19 D. Volz, D. M. Zink, T. Bocksrocker, J. Friedrichs, M. Nieger, T. Baumann, U. Lemmer and S. Brase, *Chem. Mater.*, 2013, **25**, 3414-3426.
- 20 N. Thejo Kalyani and S. J. Dhoble, *Renew. Sust. Energ. Rev.*, 2012, **16**, 2696-2723.
- 21 Y.-L. Chang, Y. Song, Z. Wang, M. G. Helander, J. Qiu, L. Chai, Z. Liu, G. D. Scholes and Z. Lu, *Adv. Funct. Mater.*, 2013, **23**, 705-712.
- 22 M. C. Gather, A. Köhnen and K. Meerholz, *Adv. Mater.*, 2011, **23**, 233-248.
- 23 M. Dong and L. Zhong, *IEEE Trans. Mobile Comput.*, 2012, **11**, 1587-1599.
- 24 J. C. Jeong, H. S. Kim and J. G. Jang, *Mol. Cryst. Liq. Cryst.*, 2010, **530**, 259-265.
- 25 P. Brulatti, V. Fattori, S. Muzzioli, S. Stagni, P. P. Mazzeo, D. Braga, L. Maini, S. Milita and M. Cocchi, *J. Mater. Chem. C*, 2013, **1**, 1823-1831.
- 26 Y.-L. Tung, P.-C. Wu, C.-S. Liu, Y. Chi, J.-K. Yu, Y.-H. Hu, P.-T. Chou, S.-M. Peng, G.-H. Lee, Y. Tao, A. J. Carty, C.-F. Shu and F.-I. Wu, *Organometallics*, 2004, **23**, 3745-3748.
- 27 D. Volz, M. Nieger, J. Friedrichs, T. Baumann and S. Brase, *Langmuir*, 2013, **29**, 3034-3044.
- 28 D. M. Zink, M. Bachle, T. Baumann, M. Nieger, M. Kuhn, C. Wang, W. Kloppe, U. Monkowius, T. Hofbeck, H. Yersin and S. Brase, *Inorg. Chem.*, 2012, **52**, 2292-2305.
- 29 J. P. Safko, J. E. Kuperstock, S. M. McCullough, A. M. Noviello, X. Li, J. P. Killarney, C. Murphy, H. H. Patterson, C. A. Bayse and R. D. Pike, *Dalton Trans.*, 2012, **41**, 11663-11674.
- 30 D. Braga, F. Grepioni, L. Maini, P. P. Mazzeo and B. Ventura, *New J. Chem.*, 2011, **35**, 339-344.
- 31 D. Braga, L. Maini, P. P. Mazzeo and B. Ventura, *Chem. - Eur. J.*, 2010, **16**, 1553-1559.
- 32 L. Maini, D. Braga, P. P. Mazzeo and B. Ventura, *Dalton Trans.*, 2012, **41**, 531-539.
- 33 M. Vitale and P. C. Ford, *Coord. Chem. Rev.*, 2001, **219-221**, 3-16.
- 34 M. Vitale, W. E. Palke and P. C. Ford, *J. Phys. Chem.*, 1992, **96**, 8329-8336.
- 35 C. K. Ryu, M. Vitale and P. C. Ford, *Inorg. Chem.*, 1993, **32**, 869-874.
- 36 C. K. Ryu, K. R. Kyle and P. C. Ford, *Inorg. Chem.*, 1991, **30**, 3982-3986.
- 37 F. De Angelis, S. Fantacci, A. Sgamellotti, E. Cariati, R. Ugo and P. C. Ford, *Inorg. Chem.*, 2006, **45**, 10576-10584.
- 38 D. Tran, J. L. Bourassa and P. C. Ford, *Inorg. Chem.*, 1997, **36**, 439-442.
- 39 A. Dossing, C. K. Ryu, S. Kudo and P. C. Ford, *J. Am. Chem. Soc.*, 1993, **115**, 5132-5137.
- 40 S. S. Batsanov, *Inorg. Mater.*, 2001, **37**, 871-885.
- 41 S. Nag, K. Banerjee and D. Datta, *New J. Chem.*, 2007, **31**, 832-834.
- 42 L. Brammer, E. A. Bruton and P. Sherwood, *Cryst. Growth Des.*, 2001, **1**, 277-290.
- 43 A. Vega and J.-Y. Saillard, *Inorg. Chem.*, 2004, **43**, 4012-4018.
- 44 A. Barbieri and G. Accorsi, *EPA Newsletters*, December 2006, 26-35.
- 45 J. R. Lakowicz, *Principle of fluorescence Spectroscopy*, Springer, New York, 3rd edn, 2006.
- 46 C. F. Macrae, I. J. Bruno, J. A. Chisholm, P. R. Edgington, P. McCabe, E. Pidcock, L. Rodriguez-Monge, R. Taylor, J. van de Streek and P. A. Wood, *J. Appl. Crystallogr.*, 2008, **41**, 466-470.
- 47 K. Shankland, W. I. F. David and D. S. Sivia, *J. Mater. Chem.*, 1997, **7**, 569-572.
- 48 G. M. Sheldrick, *SHELXL97*, University of Göttingen, Germany, 1997.
- 49 C. L. Raston and A. H. White, *J. Chem. Soc., Dalton Trans.*, 1976, 2153-2156.
- 50 V. Schramm, *Inorg. Chem.*, 1978, **17**, 714-718.